

# UC Davis

## UC Davis Previously Published Works

### Title

$\beta$ 1-adrenergic receptor O-glycosylation regulates N-terminal cleavage and signaling responses in cardiomyocytes

### Permalink

<https://escholarship.org/uc/item/1cv7004z>

### Journal

Scientific Reports, 7(1)

### ISSN

2045-2322

### Authors

Park, Misun

Reddy, Gopireddy R

Wallukat, Gerd

et al.

### Publication Date

2017

### DOI

10.1038/s41598-017-06607-z

Peer reviewed

# SCIENTIFIC REPORTS



OPEN

## $\beta_1$ -adrenergic receptor O-glycosylation regulates N-terminal cleavage and signaling responses in cardiomyocytes

Misun Park<sup>1</sup>, Gopireddy R. Reddy<sup>2</sup>, Gerd Wallukat<sup>3</sup>, Yang K. Xiang<sup>2,4</sup>  & Susan F. Steinberg<sup>1</sup>

$\beta_1$ -adrenergic receptors ( $\beta_1$ ARs) mediate catecholamine actions in cardiomyocytes by coupling to both Gs/cAMP-dependent and Gs-independent/growth-regulatory pathways. Structural studies of the  $\beta_1$ AR define ligand-binding sites in the transmembrane helices and effector docking sites at the intracellular surface of the  $\beta_1$ AR, but the extracellular N-terminus, which is a target for post-translational modifications, typically is ignored. This study identifies  $\beta_1$ AR N-terminal O-glycosylation at Ser<sup>37</sup>/Ser<sup>41</sup> as a mechanism that prevents  $\beta_1$ AR N-terminal cleavage. We used an adenoviral overexpression strategy to show that both full-length/glycosylated  $\beta_1$ ARs and N-terminally truncated glycosylation-defective  $\beta_1$ ARs couple to cAMP and ERK-MAPK signaling pathways in cardiomyocytes. However, a glycosylation defect that results in N-terminal truncation stabilizes  $\beta_1$ ARs in a conformation that is biased toward the cAMP pathway. The identification of O-glycosylation and N-terminal cleavage as novel structural determinants of  $\beta_1$ AR responsiveness in cardiomyocytes could be exploited for therapeutic advantage.

$\beta_1$ -adrenergic receptors ( $\beta_1$ ARs) are the principle mediators of catecholamine actions in cardiomyocytes.  $\beta_1$ ARs rapidly adjust cardiac output by activating a Gs-adenylyl cyclase (AC) pathway that increases cAMP, activates protein kinase A (PKA), and phosphorylates substrates involved in excitation-contraction coupling. While  $\beta_1$ ARs can also activate cardioprotective Gs-independent mechanisms via the recruitment of  $\beta$ -arrestin and transactivation of an epidermal growth factor receptor (EGFR) pathway that activates ERK<sup>1</sup>, chronic  $\beta_1$ AR activation leads to a spectrum of changes (including cardiomyocyte hypertrophy/apoptosis, interstitial fibrosis, and contractile dysfunction) that contribute to the evolution of heart failure (HF)<sup>2,3</sup>.  $\beta_1$ AR inhibitors that prevent maladaptive cAMP-driven  $\beta_1$ AR responses have become standard therapy for HF.

$\beta$ ARs have provided a useful prototype for structural and NMR spectroscopic studies designed to elucidate the molecular dynamics of G protein-coupled receptor (GPCR) activation<sup>4-6</sup>. However, studies to date have focused primarily on the human  $\beta_2$ AR, the first hormone-activated GPCR to be cloned and structurally characterized<sup>5,6</sup>. While  $\beta_1$ - and  $\beta_2$ ARs share considerable sequence homology in the transmembrane regions that form their ligand-binding pockets, other regions of these receptors are more divergent. In particular, the  $\beta_1$ - and  $\beta_2$ AR extracellular N-termini show no sequence homology. Since the  $\beta$ AR N-terminus has traditionally been viewed as having a negligible role in mechanisms that contribute to receptor activation and regulation, these relatively short and highly dynamic regions of the receptor generally are removed for structural studies. However, the notion that the  $\beta$ AR N-terminus can be dismissed as functionally unimportant is at odds with the fact that non-synonymous single nucleotide polymorphisms (SNPs) localized to the N-terminal regions of both the  $\beta_1$  and  $\beta_2$ AR function as genetic determinants of  $\beta$ AR inhibitor responses and clinical outcome in HF<sup>7</sup>.

$\beta_1$  and  $\beta_2$ AR N-termini also are targets for sugar-based modifications (i.e., glycosylation). Protein glycosylation is an abundant post-translational modification that functions to expand the diversity of the proteome. Glycosylation is subdivided into two major categories (N- or O-glycosylation) based upon the residue within the protein backbone that serves as an attachment site for the branched sugar polymer (or glycan). N-glycosylation

<sup>1</sup>Department of Pharmacology, Columbia University, New York, NY, USA. <sup>2</sup>Department of Pharmacology, University of California at Davis, Davis, CA, USA. <sup>3</sup>Experimental and Clinical Research Center, Charité Campus Buch and Max-Delbrück Center for Molecular Medicine, Berlin, Germany. <sup>4</sup>VA Northern California Health Care System, Mather, CA, USA. Correspondence and requests for materials should be addressed to S.F.S. (email: [sfs1@columbia.edu](mailto:sfs1@columbia.edu))

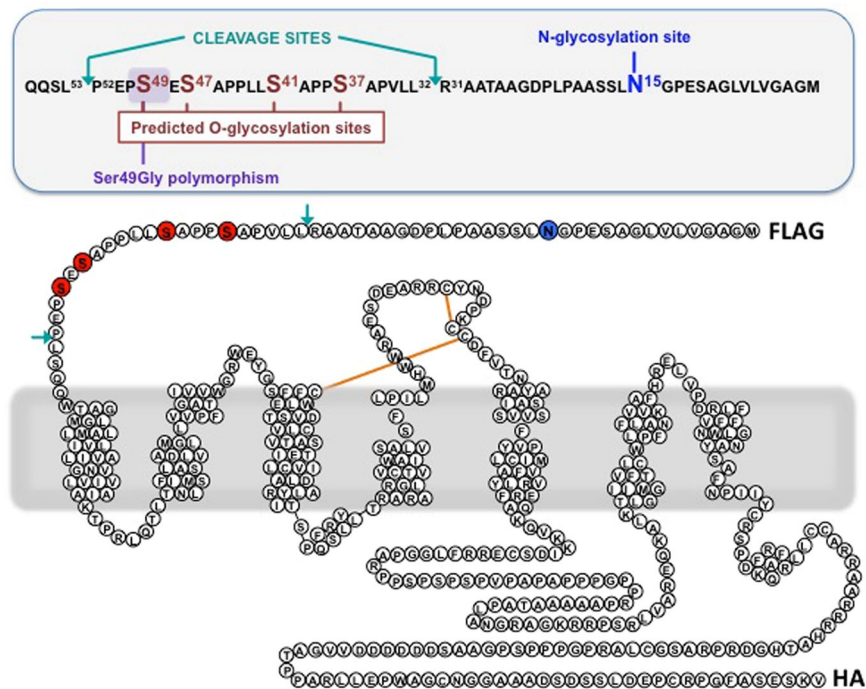


**Figure 1.** Schematic of the 2-dimensional topology of the human  $\beta_1$ AR. The single N-glycosylation site in the N-terminus at position 15, in a consensus sequence [Nx(S/T)] is shown in blue. Putative O-glycosylation consensus sites (Ser residues in a Pro-rich environment) examined in this study are shown in red; the Ser49Gly polymorphism maps to a putative O-glycosylation site. Cleavage sites previously identified at the  $\beta_1$ AR N-terminus are shown in turquoise<sup>13</sup>; cleavage at P52-L53 generates a non-glycosylated receptor. Constructs used for the experiments depicted in Figs 2, 3 and 6 contained N-terminal FLAG (DYKDDDDK) and C-terminal HA (YPYDVPDYA) tags.

is initiated in the endoplasmic reticulum by the actions of an oligosaccharide transferase which catalyzes the *en bloc* transfer of a preformed complex glycan structure to the amide nitrogen on the side chain of an asparagine residue (in a Asn-x-Ser/Thr consensus sequence - where x is any residue other than proline<sup>8</sup>). The N-linked glycan structure then undergoes extensive modification during protein transport from the Golgi to the plasma membrane. In contrast, O-glycosylation is initiated by the transfer of a single monosaccharide (generally  $\alpha$ -GalNAc) to the hydroxyl group of an acceptor serine or threonine residue<sup>8,9</sup>. This reaction (which is catalyzed by a polypeptide GalNAc-transferase, a multi-gene family of ~20 different enzymes) is then followed by the step-wise enzymatic transfer of additional sugars (including galactose, GlcNAc, and fucose) to yield a spectrum of higher order linear and branched glycan structures. Both N- and O-linked glycan structures are then typically capped with negatively charged sialic acids. Glycan structures (in some cases on specific proteins) have been implicated in a vast number of key biological processes (including protein trafficking to membranes, cell adhesion, signal transduction, endocytosis) that are critical for normal embryonic development and normal organ physiology<sup>8</sup>. Recent studies also indicate that glycan structures are highly regulated during developmental and in response to environmental stimuli (conditions that leads to changes in the relative abundance and location of individual glycosyltransferase enzymes, the abundance and trafficking of glycoprotein substrates, and/or the availability of activated sugar donors) and that disordered protein glycosylation is a common feature of various inflammatory and metabolic disorders and a hallmark of certain cancers<sup>10,11</sup>.

$\beta$ ARs have both been categorized as glycoproteins, but the number and types of glycan attachments to the  $\beta_1$ AR versus the  $\beta_2$ AR are quite different. The  $\beta_2$ AR contains 2 sites for N-linked glycosylation at its extreme N-terminus (at N<sup>6</sup>GSAFLLAPN<sup>15</sup>GS)<sup>12</sup>.  $\beta_2$ AR N-glycosylation has been implicated as a mechanism that influences  $\beta_2$ AR trafficking to cell surface membranes; it does not influence  $\beta_2$ AR ligand binding or coupling to the Gs-cAMP pathway<sup>12</sup>. In contrast, the  $\beta_1$ AR N-terminus contains a single site for N-linked glycosylation at Asn<sup>15</sup><sup>13</sup>.  $\beta_1$ AR N-glycosylation at this site is reported to influence  $\beta_1$ AR homodimerization and  $\beta_1$ AR heterodimerization with  $\alpha_2$ ARs; effects on ligand binding or agonist-induced internalization are not detected<sup>14,15</sup>. However, the  $\beta_1$ AR N-terminus also is the target for O-linked glycosylation<sup>13</sup>. Computational algorithms have been used to map this modification to a cluster of consensus O-glycosylation sites (i.e., Ser in a Pro-rich region) at S<sup>37</sup>, S<sup>41</sup>, S<sup>47</sup>, and S<sup>49</sup> (Fig. 1)<sup>13</sup>, but the specific sites within the  $\beta_1$ AR N-terminus that are targets for O-linked glycan modifications have never been unambiguously identified. This omission is pertinent, since Ser<sup>37</sup>, Ser<sup>41</sup>, and Ser<sup>47</sup> are highly conserved in mammalian  $\beta_1$ ARs, but sequence variation within the coding sequence of *ADRB1* gives rise to the Gly<sup>49</sup> allele in ~20% of Caucasian and ~15% of African Americans<sup>16</sup>. The notion that a Ser49Gly polymorphism might alter  $\beta_1$ AR O-glycosylation patterns and thereby underlie this human SNP's function as a clinically important modifier of  $\beta$ AR inhibitor responsiveness and outcome in patients with HF<sup>16</sup> has never been considered. Similarly,

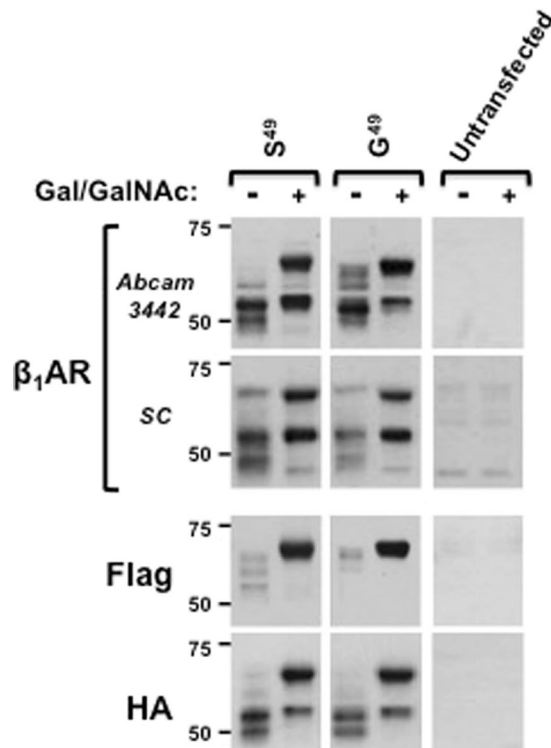


**Figure 2.** The S49G polymorphic variant does not grossly influence  $\beta_1$ AR glycosylation profiles in *ldlD* cells. Lysates from *ldlD* cells transiently transfected with plasmids that drive expression of either S<sup>49</sup>- or G<sup>49</sup>- $\beta_1$ ARs and cultured without or with Gal (20  $\mu$ M) and GalNAc (200  $\mu$ M) were subjected to immunoblot analysis with two different anti- $\beta_1$ AR antibodies as well as antibodies to Flag and HA epitope tags at the N- and C-termini, respectively. The figure shows that the Abcam anti- $\beta_1$ AR antibody (ab3442, raised against residues 394–408 in human  $\beta_1$ ARs) and the Santa Cruz anti- $\beta_1$ AR antibody (raised against some undefined C-terminal epitope) both detect the heterologously overexpressed  $\beta_1$ AR. However, immunoblots with the Santa Cruz anti- $\beta_1$ AR antibody also contain some non-specific immunoreactivity. In particular, a ~69-kDa non-specific band that comigrates with the full-length, fully glycosylated  $\beta_1$ AR can become rather problematic at low levels of transgene expression. Therefore, the Abcam reagent (which is more sensitive and specific) was used in subsequent experiments.

the consequences of  $\beta_1$ ARs O-glycosylation remain uncertain. There is evidence that clusters of O-glycans in other membrane-bound proteins alter protein secondary structure, serve as ligands for cell adhesion, and can be sources of antigen for the immune system<sup>17</sup>. Mucin-like O-glycans also have been implicated as barriers that prevent protein cleavage by proteases<sup>17</sup>, a property that might be particularly relevant the  $\beta_1$ AR since the human  $\beta_1$ AR (like its turkey counterpart) undergoes N-terminal cleavage at sites adjacent to the putative O-glycosylation sites (Fig. 1 and refs 13 and 18). This study uses molecular and biochemical strategies to map O-glycosylation sites on the  $\beta_1$ AR N-terminus and show that O-glycosylation regulates  $\beta_1$ AR cleavage, a process that in turn influences  $\beta_1$ AR signaling properties in cardiomyocytes.

## Results

**$\beta_1$ AR Glycosylation Sites.**  $\beta_1$ AR glycosylation patterns were interrogated in Chinese hamster ovary (CHO) *ldlD* cells, a cell line that is UDP-galactose/UDP-N-acetylgalactosamine 4-epimerase-deficient. *ldlD* cells cannot synthesize UDP-Gal or UDP-GalNAc, the nucleotide sugars required for the addition of galactose (Gal) and N-acetylgalactosamine (GalNAc) to N- or O-linked oligosaccharides on glycoproteins, under conventional culture conditions with glucose as the sole sugar source<sup>19</sup>. However, the 4-epimerase defect can be bypassed and oligosaccharide synthesis can be fully restored by the addition of Gal and GalNAc to the culture medium, making *ldlD* cells a unique resource to map  $\beta_1$ AR glycosylation sites.

Initial studies examined the expression patterns for WT-Ser<sup>49</sup>- $\beta_1$ ARs and WT-Gly<sup>49</sup>- $\beta_1$ ARs (the two  $\beta_1$ AR polymorphic variants, see Fig. 1) in *ldlD* cells grown without or with Gal/GalNAc. Figure 2 shows that in the absence of Gal/GalNAc, both  $\beta_1$ AR variants accumulate primarily as cleaved ~48–52-kDa species that are recognized by anti- $\beta_1$ AR and anti-HA (antibodies directed against C-terminal epitopes), but not by anti-Flag (which recognizes the N-terminal epitope tag). The very small amounts of a somewhat larger  $\beta_1$ AR species that is produced under these conditions (and is detected by both anti- $\beta_1$ AR and anti-Flag) is presumed to represent a partially glycosylated species that is produced as a result of a low level of sugar scavenging from serum glycoproteins<sup>20</sup>. Addition of Gal/GalNAc to the culture medium leads to the accumulation of two larger  $\beta_1$ AR species; a full-length ~69-kDa  $\beta_1$ AR that retains both N-terminal Flag and C-terminal HA tags and a smaller truncated form of the receptor that

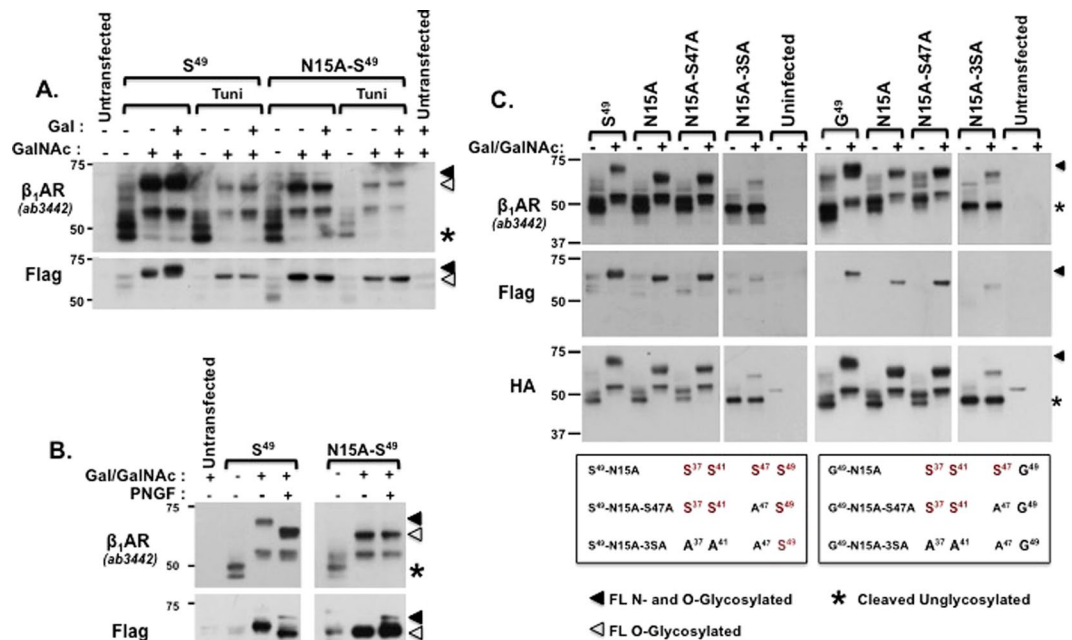


**Figure 3.** Mutagenesis studies to map  $\beta_1$ AR N-terminal glycosylation sites. *ldlD* cells transfected with wild type or single residue substituted forms of the  $\beta_1$ AR were cultured without or with Gal (20  $\mu$ M) and GalNAc (200  $\mu$ M) as indicated. Tunicamycin (Tuni) was added to the culture medium (1  $\mu$ g/ml for 24 hr) to block N-glycosylation in *Panel A*. Samples were incubated with PNGase F (PNGF 2 U/mL, 16 hr) to hydrolyze N-linked sugars in *Panel B*. Lysates were subjected to immunoblot analysis with an anti- $\beta_1$ AR antibody (raised against a  $\beta_1$ AR C-tail epitope) or antibodies to Flag and HA epitope tags at the N- and C-termini, respectively. Positions of the full-length fully N- and O-glycosylated  $\beta_1$ AR (filled triangle), the full-length O-glycosylated receptor (that lacks the N<sup>15</sup>-linked glycan, open triangle) and the N-terminally-cleaved unglycosylated receptors (asterisk) are indicated.

lacks the N-terminal Flag tag. The migration of the ~69-kDa full-length  $\beta_1$ AR is considerably slower than predicted from the calculated molecular weight of a full-length unglycosylated epitope-tagged receptor (~55-kDa) suggesting that the protein contains N- and/or O-linked glycans. Studies with Ser<sup>49</sup>- and Gly<sup>49</sup>- $\beta_1$ AR variants yielded similar results, indicating that  $\beta_1$ AR glycosylation patterns are not grossly influenced by the S49G polymorphism. It is important to note that anti- $\beta_1$ AR antibodies from two different commercial sources (Abcam 3442 and Santa Cruz sc-568) replicated the results with anti-HA; anti- $\beta_1$ AR and anti-HA antibodies detected bands with identical mobilities in transfected (but not non-transfected) cells under all experimental conditions. These results effectively address recent concerns regarding the specificity of the antibodies used to detect GPCRs such as the  $\beta$ AR<sup>21,22</sup> and indicate that these bands represent *bona fide* transgene products.

The observation that  $\beta_1$ ARs accumulate in *ldlD* cells as full-length proteins only in the presence of Gal/GalNAc indicates that glycosylation in some way prevents  $\beta_1$ AR cleavage. This could suggest a role for N- or O-linked sugars on the  $\beta_1$ AR itself, but a mechanism involving other cellular glycoconjugates is not excluded. Therefore, we mapped  $\beta_1$ AR glycosylation sites and determined whether  $\beta_1$ ARs glycosylation prevents  $\beta_1$ AR cleavage.

We first used biochemical and mutagenesis approaches to identify  $\beta_1$ AR species that contain N-linked glycans. Figures 3A and B show that the mobility of the major ~69-kDa species recognized by the anti- $\beta_1$ AR and anti-Flag antibodies increases when  $\beta_1$ ARs are synthesized in the presence of tunicamycin (which prevents N-linked chain additions) or treated with PNGase F (which specifically hydrolyzes N-linked sugars); these results indicate that the ~69-kDa band contains N-linked glycans. The smaller ~55-kDa band detected by the anti- $\beta_1$ AR antibody (but not anti-Flag) is not influenced by tunicamycin or PNGF, indicating that this is an N-terminally cleaved species and that cleavage occurs C-terminal to the N-glycosylation site. Figure 3 shows that N15A- $\beta_1$ AR is detected as N-terminally truncated ~48- and 52-kDa species in *ldlD* cells cultured without Gal/GalNAc and that  $\beta_1$ AR-N15A accumulates as two larger species in the presence of Gal/GalNAc: [1] a full length ~66-kDa species that is recognized by both anti- $\beta_1$ AR and anti-Flag antibodies - that has an electrophoretic mobility identical to WT- $\beta_1$ AR treated with tunicamycin or PNGF - and [2] a truncated ~55-kDa species that is selectively recognized by anti- $\beta_1$ AR, but not anti-Flag.  $\beta_1$ AR-N15A is not influenced by tunicamycin or PNGF treatment. These results indicate that  $\beta_1$ ARs contain a single site for N-glycosylation at position 15, that N-glycosylation is not required for full length  $\beta_1$ AR expression, and that N-glycosylation does not grossly regulate  $\beta_1$ AR N-terminal cleavage.

The observation that a N15A substitution prevents  $\beta_1$ AR N-glycosylation, but does not discernibly alter  $\beta_1$ AR processing/maturation provided the rationale to use the N-glycosylation-defective N15A- $\beta_1$ AR construct as a backbone for subsequent studies designed to identify sites for O-glycosylation. We focused on a cluster of

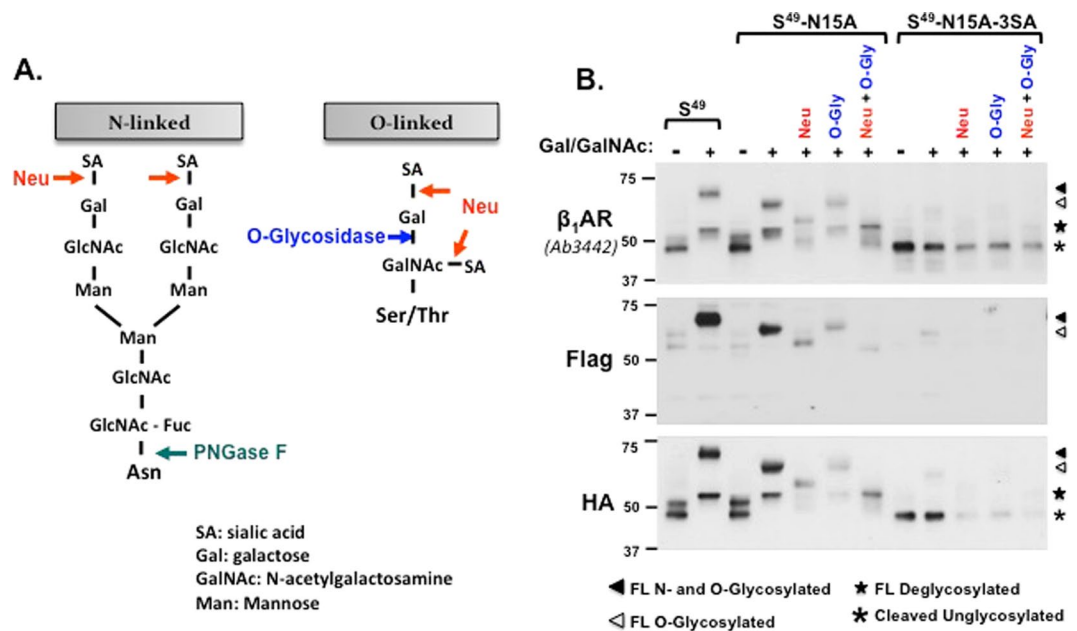


**Figure 4.**  $\beta_1$ ARs carry sialylated N- and O-linked glycans that are released by enzymatic deglycosylation. **Panel A:** Schematics showing cleavage sites in representative N- or O-linked glycan structures. Enzymatic deglycosylations were performed with Neuraminidase (Neu), O-Glycosidase (O-Gly), and Peptide-N-glycosidase F (PNGase F). **Panel B:** Lysates from *ldlD* cells transfected with S<sup>49</sup>- $\beta_1$ AR, S<sup>49</sup>- $\beta_1$ AR-N15A, or S<sup>49</sup>- $\beta_1$ AR-N15A-3SA cultured without or with Gal (20  $\mu$ M) and GalNAc (200  $\mu$ M) were subjected to deglycosylation protocols as described in Methods. Lysates were then probed with antibodies that recognize C-terminal epitopes (anti- $\beta_1$ AR and anti-HA) or N-terminal Flag. Positions of the full-length fully N- and O-glycosylated  $\beta_1$ AR (filled triangle), the full-length O-glycosylated receptor (that lacks the N<sup>15</sup>-linked glycan, open triangle), the full-length deglycosylated receptor (star), and the N-terminally-cleaved unglycosylated receptors (asterisk) are indicated.

consensus O-glycosylation sites at the juxtamembrane region of  $\beta_1$ AR N-terminus, introducing S-A substitutions at positions 37, 41, and 47 into either Ser<sup>49</sup>-N15A- $\beta_1$ AR or Gly<sup>49</sup>-N15A- $\beta_1$ AR backbones.

Figure 3C shows that the introduction of a single S47A substitution into either in the Ser<sup>49</sup>-N15A- $\beta_1$ AR or Gly<sup>49</sup>-N15A- $\beta_1$ AR background does not alter the relative abundance or the mobility of the  $\beta_1$ AR species that accumulate in *ldlD* cells cultured without or with Gal/GalNAc. These results effectively exclude Ser<sup>47</sup> and Ser<sup>49</sup> as a  $\beta_1$ AR O-glycosylation sites or sites that regulate  $\beta_1$ AR cleavage. Rather, Fig. 3C shows that  $\beta_1$ AR mutants that harbor additional S-A substitutions at positions 37 and 41 (the Ser<sup>49</sup>-N15A-3SA- $\beta_1$ AR or Gly<sup>49</sup>-N15A-3SA- $\beta_1$ AR constructs) accumulate as an N-terminally cleaved ~48-kDa species (detected by anti- $\beta_1$ AR and anti-HA, but not anti-Flag) in *ldlD* cells incubation either without or with Gal/GalNAc. These results effectively map  $\beta_1$ AR O-glycosylation sites to Ser<sup>37</sup> and/or Ser<sup>41</sup> and implicate O-glycosylation at these sites as a modification that prevents  $\beta_1$ AR N-terminal cleavage.

O-glycosylation was assessed further with neuraminidase (which removes terminal sialic acids from N- and O-linked sugars) and O-glycosidase (which removes O-linked glycan cores from glycoproteins only after the terminal sialic acid has been removed by neuraminidase). Figure 4 shows that neuraminidase treatment increases the electrophoretic mobility of N15A- $\beta_1$ ARs. Since the N15A substitution prevents  $\beta_1$ AR N-glycosylation, these results indicate that  $\beta_1$ ARs contain sialylated O-linked glycans. Treatment with O-glycosidase alone does not alter N15A- $\beta_1$ AR mobility, but the full-length ~65-kDa Ser<sup>49</sup>-N15A- $\beta_1$ AR species collapses to a ~55-kDa species following combined treatment with O-glycosidase + neuraminidase. Deglycosylation experiments performed in parallel on N15A-3SA- $\beta_1$ ARs and showed that the N15A-3SA- $\beta_1$ AR species that accumulates in Gal/GalNAc-treated *ldlD* cells is not influenced by O-glycosidase and/or neuraminidase treatments (i.e., this species is neither sialylated nor O-glycosylated). Deglycosylation experiments on the Gly<sup>49</sup> variant of the  $\beta_1$ AR harboring N15A or N15A-3SA- $\beta_1$ AR yielded identical results (data not shown). Collectively, these results indicate that  $\beta_1$ ARs accumulate as O-glycosylated species in *ldlD* cells cultured with Gal/GalNAc, that O-glycosylation sites also are heavily sialylated, and that O-linked sugar modifications at Ser<sup>37</sup> and/or Ser<sup>41</sup> prevent  $\beta_1$ AR cleavage.

Finally, these experimental protocols were replicated using an untagged  $\beta_1$ AR construct to address the possible concern that the epitope tags might influence  $\beta_1$ AR maturation/glycosylation. These additional studies were considered important since a C-terminal tag on the  $\beta_2$ AR subtype (which like the  $\beta_1$ AR, terminates in a S-x- $\phi$  class I PDZ binding motif) disrupts PDZ domain-mediated protein interactions and prevents  $\beta_2$ AR recycling to surface membranes following agonist-induced internalization<sup>23</sup>; N-terminal tags on  $\beta$ AR subtypes typically are viewed as functionally silent. Figure S1A shows that an untagged  $\beta_1$ AR construct is detected as a ~69-kDa band, corresponding to the full-length  $\beta_1$ AR, in *ldlD* cells grown with (but not without) Gal/GalNAc. Figure S1B shows that the electrophoretic mobility of this ~69-kDa band increases in response to treatment with PNGase F

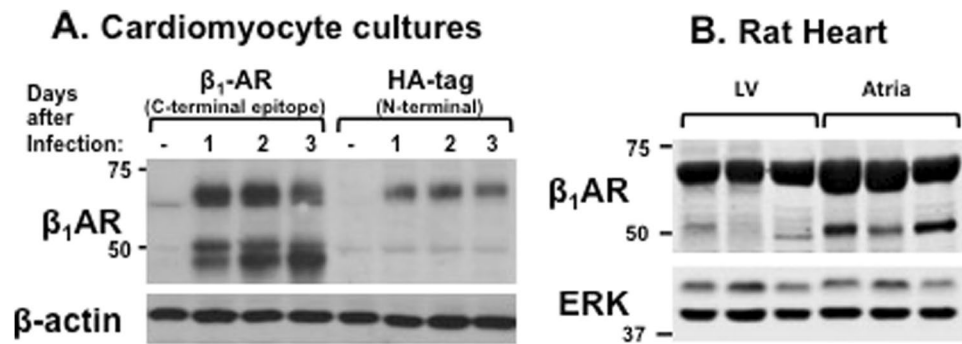


**Figure 5.**  $\beta_1$ AR are detected as full-length and truncated species in cardiomyocytes. *Panel A:* Adenoviral-mediated gene delivery was used to overexpress N-terminally tagged  $\beta_1$ ARs in neonatal rat cardiomyocyte cultures. Lysates were prepared at 1–3 days following infection and probed for  $\beta_1$ ARs, with  $\beta$ -actin used as a protein loading control. *Panel B:* Lysates prepared from adult left ventricular (LV) or atrial tissues were probed for  $\beta_1$ AR expression (with ERK protein serving as loading control, since the anti- $\beta$ -actin antibody - which gives a very robust signal in various cell culture preparations - performed poorly in lysates prepared from intact rat hearts). A shorter exposure of the  $\beta_1$ AR immunoblot is included as Fig. S2.

(indicating that it contains N-linked glycans) and that neuraminidase and O-glycosidase treatments produce further increases in this band's electrophoretic mobility over that produced by PNGase F treatment alone (indicating that it also contains sialylated O-linked glycans). The observation that the untagged  $\beta_1$ AR is processed (like the tagged  $\beta_1$ AR) to a ~69-kDa protein that contains sialylated N- and O-linked glycans in *ldld* cells grown with Gal/GalNAc establishes that the N- and C-terminal tags do not influence  $\beta_1$ AR glycosylation.

**$\beta_1$ ARs accumulate as both full-length and N-terminally cleaved species in cardiomyocytes.** We previously identified distinct molecular forms of the  $\beta_1$ AR in rat cardiomyocyte cultures and rat ventricle and concluded that these distinct molecular species represent *bona fide*  $\beta_1$ AR gene products, since similar molecular heterogeneity of  $\beta_1$ ARs is detected in the hearts of wild type mice but not  $\beta_1$ AR null mutants<sup>24,25</sup>. However, the previous immunoblotting studies relied exclusively on antibodies directed against C-terminal epitopes and could not resolve  $\beta_1$ AR mobility differences due to receptor cleavage versus other mechanisms (for example, differential glycosylation or oxidative modifications at extracellular loop cysteines that influence intramolecular disulfide bond formation)<sup>26</sup>. Therefore, adenoviral-mediated gene transfer was used to overexpress N-terminally HA-tagged  $\beta_1$ ARs in cardiomyocytes. Figure 5A shows that an antibody directed against a  $\beta_1$ AR C-terminal epitope detects the transgene as both a larger ~69-kDa and two smaller ~45–50-kDa species and that only the larger ~69-kDa species carries the N-terminal HA-tag. These results indicate that the smaller species is the product of N-terminal cleavage in cardiomyocytes. Figure 5A also shows that both full-length and truncated forms of the  $\beta_1$ AR are detected within 24 hr of adenoviral infection and their levels remain stable for up to 3 days.

Recent studies identify atrial-ventricular differences in glycosylation-associated gene (glycogene) expression that lead to chamber-specific differences in protein glycosylation<sup>27</sup>. Therefore, we performed immunoblotting as a general screen to identify tissue-specific difference in  $\beta_1$ AR processing. Figure 5B shows that  $\beta_1$ ARs are detected as a ~69-kDa species in membranes prepared from rat left ventricle and atrium and that atrium is relatively enriched in a smaller ~52-kDa species that co-migrates with the N-terminally truncated  $\beta_1$ AR.

**N-terminal truncation alters  $\beta_1$ AR signaling in cardiomyocytes.** We generated an N-terminally truncated form of the  $\beta_1$ AR based upon a cleavage site identified by N-terminal sequencing in a previous study<sup>13</sup> and packaged this construct into an adenoviral vector to drive  $\beta_1$ AR expression in cardiomyocytes. Untagged  $\beta_1$ AR constructs were packaged into adenoviral vectors for these expression studies, to avoid any possible confounding effects of the epitope tags. Preliminary radioligand binding experiments established that membranes with similar levels of either full length (FL) or N-terminally truncated  $\beta_1$ AR ( $\Delta 2$ -52- $\beta_1$ AR) immunoreactivity contain similar numbers of [<sup>125</sup>I]CYP binding sites ( $838 \pm 91$  vs.  $725 \pm 62$  fmol/mg;  $n = 4$ , NS) that bind [<sup>125</sup>I]CYP with similar affinity ( $65.5 \pm 29.4$  vs.  $77.5 \pm 15.7$  pM;  $n = 4$ , NS). The observation that an N-terminal truncation does not impair  $\beta_1$ AR interactions with an antagonist ligand is consistent with structural studies that map the  $\beta_1$ AR ligand binding pocket to residues in transmembrane helices and the second extracellular loop<sup>28</sup>.

Cardiomyocytes that heterologously overexpress similar levels of FL or N-terminally truncated  $\beta_1$ ARs were challenged with a range of isoproterenol concentrations to determine whether N-terminal cleavage alters  $\beta_1$ AR signaling to Gs/cAMP versus ERK pathways. Figure 6 shows that Ad- $\Delta 2$ -52- $\beta_1$ AR cultures display a higher level of cAMP accumulation (and reduced ERK phosphorylation) in response to a range of isoproterenol concentrations, compared to Ad-FL- $\beta_1$ AR cultures. While a previous study identified higher levels of the cleaved  $\beta_1$ AR species following long-term (6 hr) agonist activation (and concluded that  $\beta_1$ ARs are cleaved upon agonist activation<sup>13</sup>), the more short term isoproterenol treatment used in this study does not alter the abundance of any  $\beta_1$ AR species in cardiomyocytes. These results argue that the N-terminal cleavage that is detected in cardiomyocytes is a stable modification that is completed prior to the delivery of the  $\beta_1$ AR to the cell surface membrane and is not

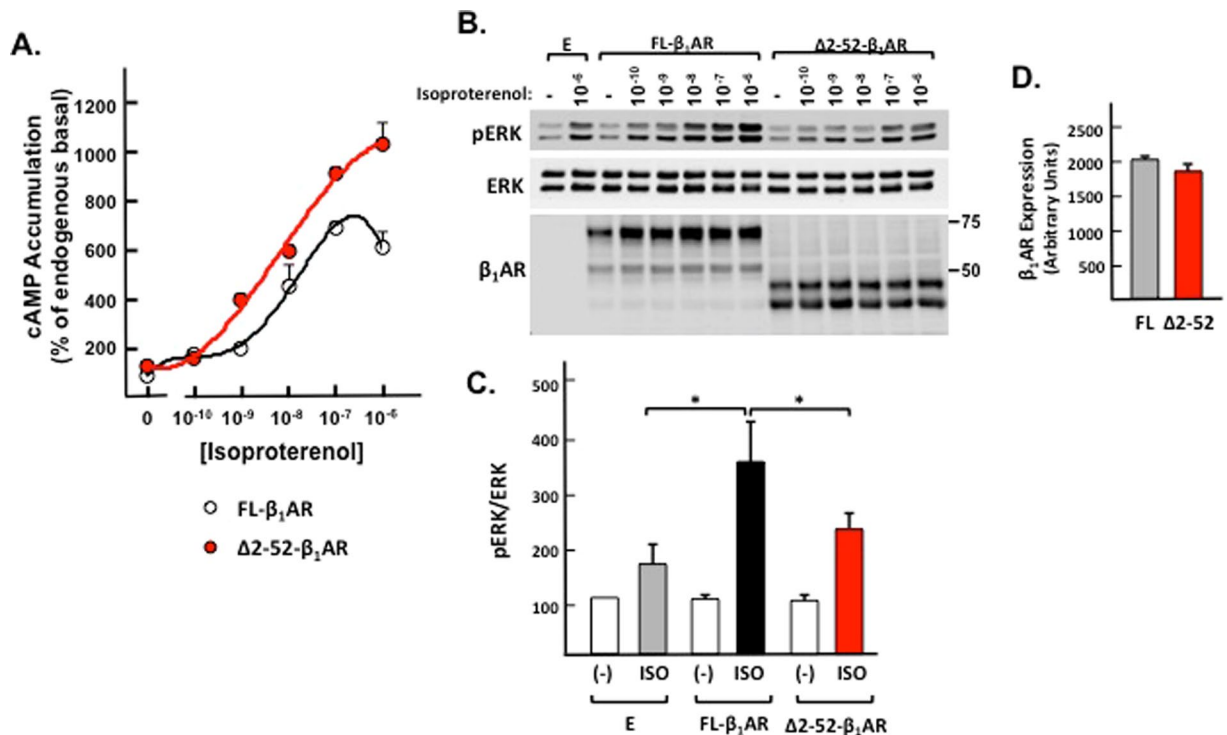


**Figure 6.** N-terminal truncation influences  $\beta_1$ AR signaling to cAMP versus ERK pathways in cardiomyocytes. Neonatal cardiomyocyte cultures were infected with empty vector (E) or adenoviruses that drive expression of FL (Ad-FL- $\beta_1$ AR) or truncated (Ad- $\Delta 2$ -52- $\beta_1$ AR) forms of the  $\beta_1$ AR. **Panel A:** Cultures were preincubated with 10 mM theophylline for 1 h at 37 °C and then challenged with vehicle or a range of isoproterenol concentrations and cAMP accumulation was measured according to Methods. Analysis by ANOVA followed by Tukey's test showed that maximal cAMP accumulation is higher in Ad- $\Delta 2$ -52- $\beta_1$ AR than in Ad-FL- $\beta_1$ AR cultures ( $p < 0.05$ ,  $n = 3$ ). **Panel B:** Lysates from cultures treated for 5 min with vehicle or a range of isoproterenol concentrations were subjected to immunoblot analysis for ERK protein and phosphorylation and  $\beta_1$ AR protein expression. **Panel C:** Quantification of pERK (normalized to ERK protein) in resting and  $10^{-6}$  M isoproterenol-treated cultures infected with empty vector, FL- $\beta_1$ AR or  $\Delta 2$ -52- $\beta_1$ AR showing that basal pERK/ERK ratios are not influenced by Ad-FL- $\beta_1$ AR or Ad- $\Delta 2$ -52- $\beta_1$ AR overexpression, but Isoproterenol-dependent ERK phosphorylation is higher in Ad-FL- $\beta_1$ AR than in Ad- $\Delta 2$ -52- $\beta_1$ AR cultures (mean  $\pm$  SEM,  $n = 6$ , \* $p < 0.05$ ). **Panel D:** FL- $\beta_1$ AR and  $\Delta 2$ -52- $\beta_1$ AR expression was quantified (by combining signals from the two immunoreactive species detected for each construct) and did not differ (mean  $\pm$  SEM,  $n = 6$ , NS).

dynamically regulated by agonist activation. Rather, our studies indicate that N-terminal cleavage functions to alter the balance of  $\beta_1$ AR signaling to the Gs/cAMP versus the ERK signaling pathway.

**$\beta_1$ AR glycosylation influences responses to agonistic autoantibodies.** Autoantibodies against the 2<sup>nd</sup> extracellular loop of the  $\beta_1$ AR accumulate in certain heart failure syndromes (Chagas' disease, dilated cardiomyopathy, ischemic cardiomyopathy) and contribute to the pathogenesis of these disorders by binding and activating the  $\beta_1$ AR. We examined whether post-translational processing events localized to the  $\beta_1$ AR N-terminus influence the  $\beta_1$ AR responsiveness to anti- $\beta_1$ AR agonistic autoantibodies (AABs). The studies took advantage of membrane-targeted A-Kinase Activity Reporter (AKAR), a FRET reporter that senses plasma membrane localized PKA activity<sup>29</sup> (a localized signal that is regulated by a local pool of cAMP and may not necessarily track the global change in cAMP accumulation detected in Fig. 6). Figure 7 shows that both isoproterenol and anti- $\beta_1$ AR AABs increase plasma membrane PKA activity in cells that express WT- $\beta_1$ AR and glycosylation-defective  $\beta_1$ AR-N15A-3SA. While the isoproterenol-dependent increase in membrane PKA activity is more robust at early time points (2–4 min) in WT- $\beta_1$ AR cells compared to  $\beta_1$ AR-N15A-3SA cells, this difference wanes with more prolonged incubations. However, at all time points, the glycosylation-defective  $\beta_1$ AR-N15A-3SA elicits a markedly exaggerated response to agonistic anti- $\beta_1$ AR AABs compared to WT- $\beta_1$ ARs. It's worth noting that the AABs were better than isoproterenol at stabilizing  $\beta_1$ AR-N15A-3SA in a conformation that activates membrane-localized PKA; a similar superior efficacy of some AABs batches - compared to isoproterenol - has been reported by others (although the notion that AABs might be particularly efficacious at only certain molecular forms of the  $\beta_1$ ARs was not previously considered)<sup>30</sup>. These results support the conclusion that  $\beta_1$ ARs are stabilized in a conformation that is biased toward the cAMP pathway as a result of defective O-glycosylation and/or the resultant N-terminal truncation.



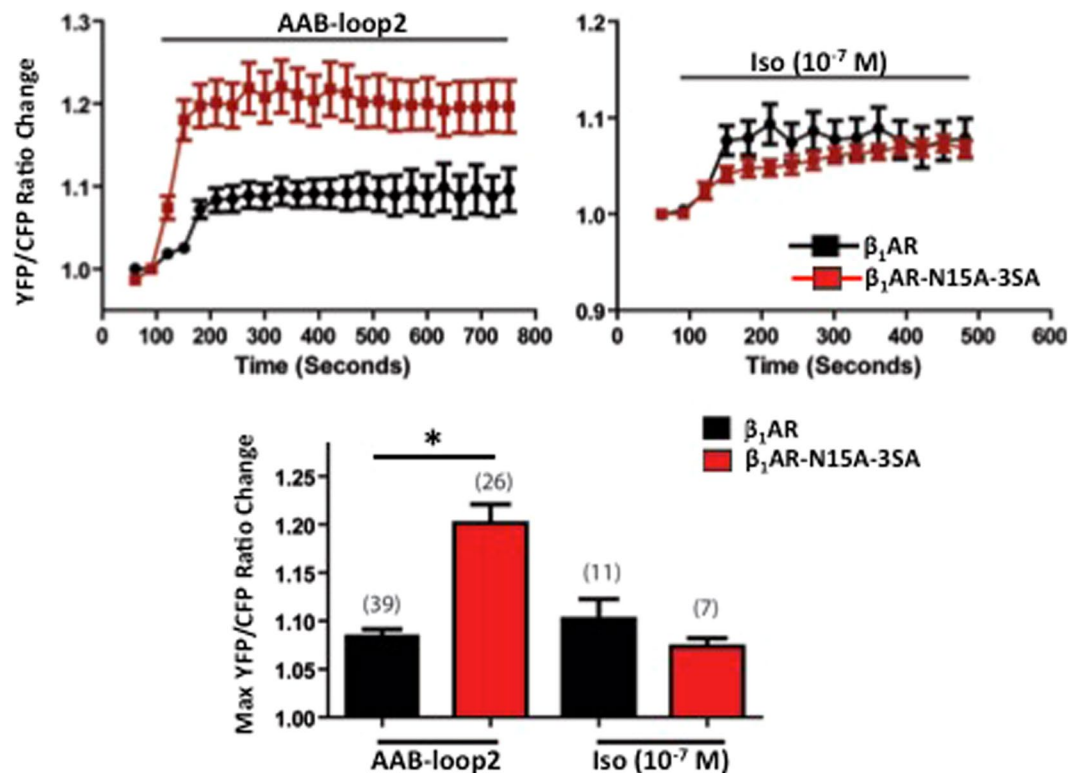


**Figure 7.**  $\beta_1$ AR O-glycosylation influences responses to agonistic autoantibodies. Neonatal rat cardiomyocytes that heterologously overexpress PM-AKAR3 (the plasma membrane-localized PKA activity FRET biosensor) plus similar amounts of either  $S^{49}$ -WT- $\beta_1$ AR or glycosylation defective  $S^{49}$ - $\beta_1$ AR-N15A-3SA were stimulated with  $\beta_1$ AR agonistic autoantibodies (AAB-loop2) or isoproterenol ( $10^{-7}$  M) and FRET was measured at 30 sec intervals. Note: The  $S^{49}$ -WT- $\beta_1$ AR and  $S^{49}$ - $\beta_1$ AR-N15A-3SA constructs used in these experiments are identical to the constructs used for the biochemical studies in Figs 2–4. *Top:* Time course for agonist-induced changes in FRET ratios (normalized to resting levels before drug). *Bottom:* Maximum FRET responses to AABs and Iso. \* $p < 0.01$  by one-way ANOVA followed by Tukey's test.

## Discussion

Protein O-glycosylation is an evolutionarily conserved mechanism that can enhance the functional diversity of a target protein. Most studies have focused on the dense clusters of GalNAc-type O-glycan modifications that decorate mucin-domains of relatively abundant secreted proteins that can be subjected to large-scale purification for analytic methods. However, recent studies suggest that GalNAc-type O-glycosylation is a more common post-translational modification that also occurs at isolated sites on a wide range of proteins without mucin-like features. Progress toward identifying these other O-glycosylation sites (and in particular, the identification of O-glycosylation sites on cell surface proteins, such as G protein-coupled receptors) and efforts to understand the functional significance of O-glycan modifications in normal development and/or the pathogenesis of various clinical disorders has lagged considerably at least in part due to several formidable technical challenges: [1] O-linked glycan structures are non-template driven modifications that characteristically shows high levels of structural diversity ('microheterogeneity'), even at a single site within a given protein. [2] Pharmacologic compounds that specifically inhibit polypeptide GalNAc transferases or enzymes that can be used to quantitatively release all O-glycan structures from protein backbones are not available. [3] The necessary and sufficient elements that comprise a consensus O-glycosylation motif remain uncertain; bioinformatics algorithms have been trained on a selective set of known O-glycoproteins and do not predict most sites identified in the human O-GalNAc glycoproteome using newly developed mass spectrometry methods<sup>31</sup>. [4] Available analytic techniques remain cumbersome and have substantial limitations. While there are isolated reports that O-glycan modifications decorate the N-termini of certain G protein-coupled receptors (V2 vasopressin, LDL, and chemokine receptors<sup>32–34</sup>) and that O-linked sugars on the LDL receptor itself (rather than on other cellular components) prevent receptor N-terminal proteolytic cleavage and stabilize LDL receptors on the cell surface<sup>33</sup>, most studies of  $\beta$ ARs have focused on the N-linked glycan modifications that can be detected on both  $\beta_1$ AR and  $\beta_2$ ARs. The O-glycan modifications that are confined to  $\beta_1$ ARs are seldom considered. This study maps  $\beta_1$ AR O-glycosylation sites and implicates O-glycosylation as a mechanism that prevents  $\beta_1$ AR N-terminal cleavage and influences  $\beta_1$ AR signaling responses in cardiomyocytes.

We used a mutagenesis approach to show that  $\beta_1$ AR O-glycosylation is confined to Ser<sup>37</sup>/Ser<sup>41</sup> and does not involve Ser<sup>49</sup>, the site of a clinical relevant SNP<sup>35</sup>. This result is seemingly at odds with a previous report from the Liggett laboratory, which identified distinct electrophoretic mobilities for Ser<sup>49</sup>- and Gly<sup>49</sup>- $\beta_1$ ARs stably

overexpressed in clonal CHW lines and speculated that this difference reflects a indirect/long-range effect of the position 49 polymorphism to alter  $\beta_1$ AR N-glycosylation at Asn<sup>15</sup>; a role for Ser<sup>49</sup> O-glycosylation was not considered<sup>36</sup>. In fact, we obtained these clonal cell lines from the Liggett laboratory and replicated their findings; we believe that the distinct migration patterns for Ser<sup>49</sup>- and Gly<sup>49</sup>- $\beta_1$ ARs in the clonal cell lines generated in the Liggett laboratory can be attributed to the presence of some inopportune genetic alteration (at the level of the  $\beta_1$ AR itself or some other protein that influences  $\beta_1$ AR maturation/post-translational processing) in one of their clonal cells lines, since the electrophoretic mobilities of Ser<sup>49</sup>- and Gly<sup>49</sup>- $\beta_1$ ARs stably overexpressed in clonal lines generated in our laboratory or transiently overexpressed in a range of other cell types do not differ. Rather, our studies effectively exclude a role for Ser<sup>49</sup> as a direct substrate for O-linked glycosylation or an indirect regulator of N-glycosylation.

We used a number of strategies to examine the functional consequences of  $\beta_1$ AR O-glycosylation. First, we showed that O-glycosylation is required for full-length  $\beta_1$ AR expression;  $\beta_1$ ARs accumulate as N-terminally truncated forms as a result of the O-glycosylation defect that results from Gal/GalNAc deprivation in *ldld* cells or site-directed mutagenesis. There is precedent for this type of interplay between O-glycosylation and proteolytic cleavage, with site-specific O-glycosylation at juxtamembrane regions of certain other membrane proteins (in some cases regulated by specific ppGalNAc-T isoforms with tissue-restricted patterns of expression) conferring structural stability and protecting against proteolytic cleavage (i.e., preventing ectodomain shedding)<sup>37</sup>. The identification of an O-glycosylation/N-terminal cleavage mechanism that gives rise to distinct molecular forms of the  $\beta_1$ AR provides the first credible explanation for the molecular heterogeneity displayed by native  $\beta_1$ ARs in various cardiac preparations; the endogenous  $\beta_1$ AR in cardiomyocyte cultures and mouse ventricle is detected as two distinct species, a larger ~69-kDa band (corresponding to the full-length/glycosylated receptor) and a smaller ~50-kDa band (that co-migrates with the N-terminally truncated  $\beta_1$ AR).

An O-glycosylation regulated event that regulates  $\beta_1$ AR processing is predicted to have important functional implications since the cardiac glycome is extensively remodeled during normal ventricular developmental and in the setting of cardiac hypertrophy<sup>27, 38, 39</sup>. It is interesting to speculate that developmental- or disease-associated changes in the relative abundance of ppGalNAcT family enzymes that initiate O-glycosylation, the repertoire of glycosyltransferase enzymes that extend the core O-glycan structure (that produce diverse ensembles of branched glycan structures), or the expression of sialyltransferase enzymes that cap O- and N-linked glycans with sialic acid might impact on  $\beta_1$ AR glycosylation (and secondarily  $\beta_1$ AR cleavage and  $\beta_1$ AR responsiveness). The observation that glycan-modifying enzyme expression and protein glycosylation patterns are regulated in a tissue-specific manner (including between atrial *versus* ventricular tissues<sup>27</sup>) provides a likely explanation for the atrial-ventricular difference in the abundance of the smaller molecular form of the  $\beta_1$ AR that co-migrates with N-terminally truncated  $\beta_1$ ARs. Collectively, these results provide a strong rationale to consider functionally-important glycosylation-driven changes in  $\beta_1$ AR structure as a dynamically regulated mechanism that contributes to the pathogenesis of various cardiac phenotypes. However, an analysis of site-specific glycan modifications on native  $\beta_1$ ARs in various cardiac tissues (to characterize the structural changes in O-glycan moieties that accompany or contribute to the pathogenesis of cardiac diseases) remains technically challenging even with the most contemporary O-glycoproteomic methods (see ref 40). More sophisticated analytic strategies that can be used to dissect glycan structural diversity, particularly on native O-glycoproteins in complex biological samples, are under development and will be critical for future progress in this area.

Our studies identify an O-glycosylation-regulated N-terminal cleavage event as a mechanism that alters  $\beta_1$ AR signaling bias to cAMP/PKA versus ERK pathways. With the caveat that the functional studies were performed in overexpression models (and ultimately must be followed-up by studies that interrogate glycosylation/cleavage mechanisms that control the expression and action of native  $\beta_1$ ARs at endogenous levels of  $\beta_1$ AR expression), these studies suggest that an O-glycosylation-regulated mechanism that dictates  $\beta_1$ AR responsiveness could underlie the cardiac phenotypes that develop in various syndromes associated with defective in glycoprotein glycosylation. For example, congenital disorders of glycosylation due to mutations or deletion of genes that encode the enzymes that form the core O-glycan structures typically present with lethal ventricular arrhythmias and cardiomyopathies<sup>41</sup>. The molecular basis for this glycosylation-driven cardiac phenotype remains uncertain. Studies to date have linked defects in protein glycosylation (that disrupt protein sialylation) to changes in the gating properties of certain voltage-gated sodium and potassium channels, enhanced cardiac excitability, and increased susceptibility to ventricular arrhythmias<sup>27, 42–44</sup>. While changes in ion channel sialylation may contribute to the pathogenesis of the ventricular arrhythmias in these disorders, our studies provide a rationale to consider whether defective  $\beta_1$ AR O-glycosylation and the accumulation of an N-terminally truncated  $\beta_1$ AR species that displays enhanced signaling to proarrhythmic cAMP/PKA responses also might contribute to this pathologic cardiac phenotype.

Ventricular arrhythmias also are a characteristic feature of acquired disorders of protein sialylation, such as Chagas disease. *Trypanosoma cruzi* (the causative agent of Chagas disease) releases a trans-sialidase that transfers sialic acid from glycoconjugates on the host cell to mucin-like proteins on the parasite cell surface. This results in changes in immune cell sialylation that effectively subvert some aspects of the host cell immune response<sup>45, 46</sup>. Of note, early studies linked *Trypanosoma cruzi* infection to changes in  $\beta$ AR responsiveness that in some cases correlate with the severity of chagasic cardiomyopathy<sup>47–49</sup>. The prevailing notion is that the disordered immune response leads to the generation of agonistic anti- $\beta_1$ AR autoantibodies that activate the cAMP signaling pathway and contribute to chagasic cardiomyopathy. While there is direct evidence that agonistic anti- $\beta_1$ AR autoantibody treatment results in a cardiomyopathic phenotype<sup>50</sup>, the limited correlation between circulating levels of anti- $\beta_1$ AR autoantibodies and the severity of cardiac dysfunction<sup>51</sup> suggests that other mechanisms also may be contributory. Our studies provide the rationale to consider whether a *Trypanosoma cruzi* infection induced decrease in  $\beta_1$ AR sialylation might facilitate  $\beta_1$ AR N-terminal cleavage, enhance agonistic antibody-dependent

activation of the cAMP/PKA pathway (while dampening signaling via the cardioprotective ERK pathway), and promote adverse cardiac remodeling.

Finally, our studies identify the  $\beta_1$ AR extracellular N-terminus as a heretofore unrecognized structural determinant of  $\beta_1$ AR responsiveness. The notion that a glycan-regulated event localized to the N-terminus can influence  $\beta_1$ AR responsiveness represents a paradigm shift from previous research that focused almost exclusively on the ligand binding sites in transmembrane helices or effector docking sites in the intracellular loops and the C-terminus. However, our results resonate with a small but growing literature that link structural perturbations (and/or changes in glycosylation) localized to the N-terminus to altered GPCR cell surface expression or compartmentation to lipid raft microdomains, changes in the kinetics of ligand-induced internalization, changes in the efficiency of receptor dimerization, and altered signaling bias to downstream effectors<sup>14, 52, 53</sup>. The identification of an O-glycan-regulated cleavage event that regulates  $\beta_1$ AR signaling to cAMP/PKA vs ERK provides a strong rationale for future studies that identify the O-glycan modifying enzymes and specific protease(s) that execute these post-translational modifications at the  $\beta_1$ AR N-terminus and the specific role of glycan-mediated changes in  $\beta_1$ AR structure/function in the pathogenesis of various cardiac disorders. The identification of O-glycosylation and/or receptor cleavage sites that are specific to the  $\beta_1$ AR N-terminus, that add plasticity to catecholamine-dependent signaling responses, could represent promising novel targets for  $\beta_1$ -subtype specific therapeutics.

**Note.** While this manuscript was under revision, a publication from Goth et al. described the sites and functional consequences of beta1-adrenergic receptor O-glycosylation (JBC 292:4714,2017). We believe that methodologic differences explain certain discrepancies between the findings in this recent publication and the results reported herein. First, Goth et al. used in vitro O-glycosylation assays with peptides based upon the  $\beta_1$ -adrenergic receptor N-terminus and recombinantly expressed GalNAc-transferase 2 to identify O-glycosylation at Ser37/Ser41 and Ser47/Ser49. Our studies, which show that Ser47 and Ser49 are not O-glycosylated in vivo in GalNAc-transferase 2-expressing ldlD-CHO cells, suggest that the in vitro approach is too promiscuous to be used as a surrogate to predict in vivo O-glycosylation sites on the full length  $\beta_1$ -adrenergic receptor protein. Second, Goth et al. linked an O-glycosylation defect to a decrease in Iso-dependent cAMP accumulation. However, this conclusion was based on studies in  $\beta_1$ -adrenergic receptor-expressing GalNac-T2/T3 knock-out HEK293 cells and may be misleading, since this cell model has a generalized defect in O-glycosylation of  $\beta_1$ -adrenergic receptors, adenylyl cyclase, and a wide array of other cellular proteins. Our studies show that the truncated/glycosylation-defective  $\beta_1$ -adrenergic receptor couples to enhanced cAMP accumulation in cardiomyocytes (a physiologically relevant cell type).

## Materials and Methods

**Materials.** Antibodies were from the following sources: anti- $\beta_1$ AR (clone V-19, which was raised against a peptide that maps to the C-terminus of the mouse  $\beta_1$ AR) and anti-HA (clone Y-11) were from Santa Cruz Biotechnology (Dallas, TX). Anti- $\beta_1$ AR (ab3442, raised against residues 394–408 in human  $\beta_1$ -ARs) and anti- $\beta$ -actin were from Abcam (Cambridge, MA). Anti-Flag M2 antibody was from Sigma-Aldrich (Saint Louis, MO). Antibodies that recognize ERK protein and phosphorylation were from Cell Signaling Technology (Danvers, MA). Goat anti-rabbit and goat anti-mouse IgG (H + L)-Horse radish peroxidase conjugates were from Bio-Rad Laboratories, Inc. (Hercules, CA). Peptide-N-glycosidase F (PNGF), O-glycosidase (O-Gly), neuraminidase (Neu), propranolol, isoproterenol (Iso), and tunicamycin were obtained from Sigma-Aldrich (Saint Louis, MO). All other chemicals were reagent grade.

**Plasmids.** A plasmid that drives expression of the human S<sup>49</sup>R<sup>389</sup>- $\beta_1$ AR harboring an N-terminal Flag-tag and C-terminal HA-tag was from Addgene. The various single residue substituted  $\beta_1$ AR mutant constructs used in this study were generated using the QuikChange mutagenesis system (Agilent Technologies). A plasmid that drives expression of the N-terminally truncated human  $\beta_1$ AR (GenBank<sup>TM</sup> accession number P08588) ( $\Delta$ 2-52- $\beta_1$ AR) harboring a C-terminal Flag tag was kindly provided by Dr. Ulla E. Petäjä-Repo from University of Oulu, Finland<sup>54</sup>. Adenoviruses that drive expression of the full-length and N-terminally truncated forms of the human  $\beta_1$ AR (Ad-FL- $\beta_1$ AR and Ad- $\Delta$ 2-52- $\beta_1$ AR) were prepared by Welgen Inc. (Worcester, MA).

**HEK293 and ldlD cell culture and transfection.** HEK293 cells were cultured in DMEM (Gibco life technologies) containing 10% FBS, 100 units/ml penicillin-streptomycin, and 2mM L-glutamine. ldlD cells were cultured in DMEM/F-12 (Ham) (1:1) (Gibco life technologies) with 10% FBS and 100 units/ml penicillin-streptomycin either without or with Gal (20  $\mu$ M) and GalNAc (200  $\mu$ M). Cell transfections were performed with the Effectene Transfection reagent (Qiagen) according to manufacturer's instructions.

**Neonatal Cardiomyocyte Culture and Adenoviral Infections.** Cardiomyocytes were isolated from the hearts of 2-day-old Wistar rats and infected with adenoviral constructs that drive expression of full length or N-terminally truncated  $\beta_1$ ARs according to methods published previously<sup>55, 56</sup>. All procedures were performed in accordance with the *Guide for the Care and Use of Laboratory Animals published by the US National Institutes of Health* (NIH Publication, 8th Edition, 2011) and were approved by the Columbia University Institutional Animal Care and Use Committee (protocol AC-AAAH6903).

**Immunoblotting.** Immunoblotting was performed on cell extracts according to methods described previously or manufacturer's instructions<sup>55</sup>. The dilutions for primary and secondary antibodies were as follows: Abcam anti- $\beta_1$ AR (ab3442) at 1:3000 followed by secondary goat anti-rabbit IgG at 1:5000; Santa Cruz anti- $\beta_1$ AR (clone V-19) at 1:1000 followed by secondary goat anti-rabbit IgG at 1:2000; anti-HA (Y-11) at 1:3000 followed by secondary goat anti-rabbit IgG at 1:5000; anti-Flag M2 at 1:700 followed by secondary goat anti-mouse IgG at

1:1000; anti-pERK at 1:2000 followed by secondary goat anti-rabbit IgG at 1:3000; anti-ERK at 1:3000 followed by secondary goat anti-rabbit IgG at 1:5000; anti- $\beta$ -actin at 1:2500 followed by secondary goat anti-mouse IgG at 1:4000. Each panel in each figure represents the results from a single gel (exposed for a uniform duration); detection was with enhanced chemiluminescence or LI-COR Odyssey CLx imaging system (LI-COR Biosciences) with image Studio Lite Ver 5.0 software used for quantification of protein expression. All results were replicated in at least three experiments on separate culture preparations.

**Enzymatic deglycosylation.** Samples were deglycosylated by preincubation with peptide-N-glycosidase F (PNGase F), O-glycosidase (O-Gly),  $\alpha$ -(2  $\rightarrow$  3, 6, 8, 9)-neuraminidase (Sialidase A, Neu) for overnight at 37 °C using Enzymatic Protein Deglycosylation Kit (EDEGLY kit, Sigma) according to manufacturer's instructions.

**Measurements of  $\beta$ AR affinity and cAMP accumulation.** Radioligand binding experiments with [<sup>125</sup>I]ICYP were performed on membrane preparations according to methods published previously<sup>57</sup>. cAMP accumulation was measured according to standard methods as described previously<sup>58</sup>. In brief, cells cultured in 6-well plates, infected with adenoviral constructs, and then 3 days later preincubated with 10 mM theophylline for 60 min and challenged for 5 min with vehicle or Iso. Assays were terminated by aspiration of the incubation buffer and addition of 0.5 mL of 100% ice-cold ethanol to each well. Cell lysates were dried in a spin vacuum and cAMP in the residue was quantified with a commercially available cAMP enzyme-linked immunosorbent assay kit (R&D Systems, Minneapolis, MN) according to manufacturer's instructions.

**Fluorescent Resonance Energy Transfer (FRET) Measurements to track sarcolemmal PKA activity.** Neonatal cardiomyocyte cultures were infected with PM-AKAR3 (a plasma membrane-targeted PKA activity reporter) according to methods described previously<sup>29</sup>. Images were acquired using a Leica DMI3000B inverted fluorescence microscope (Leica Biosystems, Buffalo Grove, IL) with a 40X oil-emersion objective lens and a charge-coupled device camera controlled by Metafluor software (Molecular Devices, Sunnyvale, CA). FRET was recorded by exciting the donor fluorophore at 430–455 nm and measuring emission fluorescence with two filters (475DF40 for cyan and 535DF25 for yellow). Images were subjected to background subtraction, and were acquired every 20 seconds with exposure time of 200 ms. The donor/acceptor FRET ratio was calculated and normalized to the ratio value of baseline. The binding of cAMP to AKAR3 increases YFP/CFP FRET ratio<sup>59</sup>.

**Statistics.** Results are shown as mean  $\pm$  SEM and were analyzed by Student's *t* test or ANOVA for multiple comparisons, with *P* < 0.05 considered statistically significant.

## References

- Noma, T. *et al.*  $\beta$ -Arrestin-mediated  $\beta_1$ -adrenergic receptor transactivation of the EGFR confers cardioprotection. *J Clin Invest* **117**, 2445–2458 (2007).
- Port, J. D. & Bristow, M. R. Altered  $\beta$ -adrenergic receptor gene regulation and signaling in chronic heart failure. *J Mol Cell Cardiol* **33**, 887–905 (2001).
- Lohse, M. J., Engelhardt, S. & Eschenhagen, T. What is the role of  $\beta$ -adrenergic signaling in heart failure? *Circ Res* **93**, 896–906 (2003).
- Bokoch, M. P. *et al.* Ligand-specific regulation of the extracellular surface of a G-protein-coupled receptor. *Nature* **463**, 108–112 (2010).
- Rosenbaum, D. M. *et al.* GPCR engineering yields high-resolution structural insights into  $\beta_2$ -adrenergic receptor function. *Science* **318**, 1266–1273 (2007).
- Rasmussen, S. G. *et al.* Crystal structure of the human  $\beta_2$ -adrenergic G-protein-coupled receptor. *Nature* **450**, 383–387 (2007).
- Dorn, G. W. 2nd & Liggett, S. B. Pharmacogenomics of  $\beta$ -adrenergic receptors and their accessory signaling proteins in heart failure. *Clin Transl Sci* **1**, 255–262 (2008).
- Stanley, P. What have we learned from glycosyltransferase knockouts in mice? *J Mol Biol* **428**, 3166–3182 (2016).
- Tian, E. & Ten Hagen, K. G. Recent insights into the biological roles of mucin-type O-glycosylation. *Glycoconj J* **26**, 325–334 (2009).
- Tran, D. T. & Ten Hagen, K. G. Mucin-type O-glycosylation during development. *J Biol Chem* **288**, 6921–6929 (2013).
- Kailemia, M. J., Park, D. & Lebrilla, C. B. Glycans and glycoproteins as specific biomarkers for cancer. *Anal Bioanal Chem* **409**, 395–410 (2017).
- Rands, E. *et al.* Mutational analysis of  $\beta$ -adrenergic receptor glycosylation. *J Biol Chem* **265**, 10759–10764 (1990).
- Hakalahti, A. E. *et al.* Human  $\beta_1$ -adrenergic receptor is subject to constitutive and regulated N-terminal cleavage. *J Biol Chem* **285**, 28850–28861 (2010).
- He, J., Xu, J., Castleberry, A. M., Lau, A. G. & Hall, R. A. Glycosylation of  $\beta_1$ -adrenergic receptors regulates receptor surface expression and dimerization. *Biochem Biophys Res Commun* **297**, 565–572 (2002).
- Xu, J. *et al.* Heterodimerization of  $\alpha_{2A}$  and  $\beta_1$ -adrenergic receptors. *J Biol Chem* **278**, 10770–10777 (2003).
- Liggett, S. B. Pharmacogenomics of  $\beta_1$ -adrenergic receptor polymorphisms in heart failure. *Heart Fail. Clin.* **6**, 27–33 (2010).
- Hang, H. C. & Bertozzi, C. R. The chemistry and biology of mucin-type O-linked glycosylation. *Bioorg Med Chem* **13**, 5021–5034 (2005).
- Jurss, R., Hekman, M. & Helmreich, E. J. Proteolysis-associated deglycosylation of  $\beta_1$ -adrenergic receptor in turkey erythrocytes and membranes. *Biochemistry* **24**, 3349–3354 (1985).
- Kingsley, D. M., Kozarsky, K. F., Hobbie, L. & Krieger, M. Reversible defects in O-linked glycosylation and LDL receptor expression in a UDP-Gal/UDP-GalNAc 4-epimerase deficient mutant. *Cell* **44**, 749–759 (1986).
- Kozarsky, K. F., Call, S. M., Dower, S. K. & Krieger, M. Abnormal intracellular sorting of O-linked carbohydrate-deficient interleukin-2 receptors. *Mol Cell Biol* **8**, 3357–3363 (1988).
- Hamdani, N. & van der Velden, J. Lack of specificity of antibodies directed against human  $\beta$ -adrenergic receptors. *Naunyn-Schmiedeberg's Arch Pharmacol* **379**, 403–407 (2009).
- Kirkpatrick, P. Specificity concerns with antibodies for receptor mapping. *Nat Rev Drug Discov* **8**, 278 (2009).
- Cao, T. T., Deacon, H. W., Reczek, D., Bretscher, A. & von Zastrow, M. A kinase-regulated PDZ-domain interaction controls endocytic sorting of the  $\beta_2$ -adrenergic receptor. *Nature* **401**, 286–290 (1999).
- Rybin, V. O., Xu, X., Lisanti, M. P. & Steinberg, S. F. Differential targeting of  $\beta$ -adrenergic receptor subtypes and adenylyl cyclase to cardiomyocyte caveolae. *J Biol Chem* **275**, 41447–41457 (2000).

25. Rohrer, D. K. *et al.* Targeted disruption of the mouse  $\beta_1$ -adrenergic receptor gene: developmental and cardiovascular effects. *Proc Natl Acad Sci USA* **93**, 7375–7380 (1996).
26. Moxham, C. P., Ross, E. M., George, S. T. & Malbon, C. C.  $\beta$ -adrenergic receptors display intramolecular disulfide bridges *in situ*: analysis by immunoblotting and functional reconstitution. *Mol Pharm* **33**, 486–492 (1988).
27. Montpetit, M. L. *et al.* Regulated and aberrant glycosylation modulate cardiac electrical signaling. *Proc Natl Acad Sci USA* **106**, 16517–16522 (2009).
28. Warne, T., Edwards, P. C., Leslie, A. G. & Tate, C. G. Crystal structures of a stabilized  $\beta_1$ -adrenoceptor bound to the biased agonists bucindolol and carvedilol. *Structure* **20**, 841–849 (2012).
29. Liu, S. *et al.* Phosphodiesterases coordinate cAMP propagation induced by two stimulatory G protein-coupled receptors in hearts. *Proc Natl Acad Sci USA* **109**, 6578–6583 (2012).
30. Bornholz, B. *et al.* Impact of human autoantibodies on  $\beta_1$ -adrenergic receptor conformation, activity, and internalization. *Cardiovasc Res* **97**, 472–480 (2013).
31. Steentoft, C. *et al.* Precision mapping of the human O-GalNAc glycoproteome through SimpleCell technology. *EMBO J* **32**, 1478–1488 (2013).
32. Sadeghi, H. & Birnbaumer, M. O-Glycosylation of the V2 vasopressin receptor. *Glycobiology* **9**, 731–737 (1999).
33. Kozarsky, K., Kingsley, D. & Krieger, M. Use of a mutant cell line to study the kinetics and function of O-linked glycosylation of low density lipoprotein receptors. *Proc Natl Acad Sci USA* **85**, 4335–4339 (1988).
34. Szpakowska, M. *et al.* Function, diversity and therapeutic potential of the N-terminal domain of human chemokine receptors. *Biochem Pharmacol* **84**, 1366–1380 (2012).
35. Dorn, G. W. 2nd & Liggett, S. B. Mechanisms of pharmacogenomic effects of genetic variation within the cardiac adrenergic network in heart failure. *Mol Pharmacol* **76**, 466–480 (2009).
36. Rathz, D. A., Brown, K. M., Kramer, L. A. & Liggett, S. B. Amino acid 49 polymorphisms of the human  $\beta_1$ -adrenergic receptor affect agonist-promoted trafficking. *J Cardiovasc Pharm* **39**, 155–160 (2002).
37. Goth, C. K. *et al.* A systematic study of modulation of ADAM-mediated ectodomain shedding by site-specific O-glycosylation. *Proc Natl Acad Sci USA* **112**, 14623–14628 (2015).
38. Rong, J. *et al.* Glycan imaging in intact rat hearts and glycoproteomic analysis reveal the upregulation of sialylation during cardiac hypertrophy. *J Am Chem Soc* **136**, 17468–17476 (2014).
39. Yang, S. *et al.* Integrated glycoprotein immobilization method for glycopeptide and glycan analysis of cardiac hypertrophy. *Anal Chem* **87**, 9671–9678 (2015).
40. Levery, S. B. *et al.* Advances in mass spectrometry driven O-glycoproteomics. *Biochim Biophys Acta* **1850**, 33–42 (2015).
41. Hennet, T. & Cabalzar, J. Congenital disorders of glycosylation: a concise chart of glycolyx dysfunction. *Trends Biochem Sci* **40**, 377–384 (2015).
42. Schwetz, T. A., Norring, S. A., Ednie, A. R. & Bennett, E. S. Sialic acids attached to O-glycans modulate voltage-gated potassium channel gating. *J Biol Chem* **286**, 4123–4132 (2011).
43. Ednie, A. R., Horton, K. K., Wu, J. & Bennett, E. S. Expression of the sialyltransferase, ST3Gal4, impacts cardiac voltage-gated sodium channel activity, refractory period and ventricular conduction. *J Mol Cell Card* **59**, 117–127 (2013).
44. Ufret-Vincenty, C. A. *et al.* Role of sodium channel deglycosylation in the genesis of cardiac arrhythmias in heart failure. *J Biol Chem* **276**, 28197–28203 (2001).
45. Freire-de-Lima, L. *et al.* Trypanosoma cruzi subverts host cell sialylation and may compromise antigen-specific CD8+ T cell responses. *J Biol Chem* **285**, 13388–13396 (2010).
46. Freire-de-Lima, L., Fonseca, L. M., Oeltmann, T., Mendonca-Previato, L. & Previato, J. O. The trans-sialidase, the major Trypanosoma cruzi virulence factor: Three decades of studies. *Glycobiology* **25**, 1142–1149 (2015).
47. Morris, S. A. *et al.* Myocardial  $\beta$ -adrenergic adenylate cyclase complex in a canine model of chagasic cardiomyopathy. *Circ Res* **69**, 185–195 (1991).
48. Morris, S. A., Tanowitz, H. B., Rowin, K. S., Wittner, M. & Bilezikian, J. P. Alteration of the pattern of  $\beta$ -adrenergic desensitization in cultured L6E9 muscle cells infected with Trypanosoma cruzi. *Mol Biochem Parasitol* **13**, 227–234 (1984).
49. Nussinovitch, U. & Shoefeld, Y. The clinical significance of anti- $\beta_1$ -adrenergic receptor autoantibodies in cardiac disease. *Clin Rev Allergy Immunol* **44**, 75–83 (2013).
50. Jahns, R. *et al.* Direct evidence for a  $\beta_1$ -adrenergic receptor-directed autoimmune attack as a cause of idiopathic dilated cardiomyopathy. *J Clin Invest* **113**, 1419–1429 (2004).
51. Talvani, A. *et al.* Levels of anti-M2 and anti- $\beta_1$  autoantibodies do not correlate with the degree of heart dysfunction in Chagas' heart disease. *Microbes Infect* **8**, 2459–2464 (2006).
52. Marada, S. *et al.* Functional divergence in the role of N-linked glycosylation in smoothened signaling. *PLoS Genet* **11**, e1005473 (2015).
53. Cho, D. I. *et al.* The N-terminal region of the dopamine D2 receptor, a rhodopsin-like GPCR, regulates correct integration into the plasma membrane and endocytic routes. *Br J Pharmacol* **166**, 659–675 (2012).
54. Hakalahti, A. E. *et al.*  $\beta$ -adrenergic agonists mediate enhancement of  $\beta_1$ -adrenergic receptor N-terminal cleavage and stabilization *in vivo* and *in vitro*. *Mol Pharmacol* **83**, 129–141 (2013).
55. Ozgen, N. *et al.* Protein kinase D links Gq-coupled receptors to cAMP response element-binding protein (CREB)-Ser<sup>133</sup> phosphorylation in the heart. *J Biol Chem* **283**, 17009–17019 (2008).
56. Steinberg, S. F., Robinson, R. B., Lieberman, H. B., Stern, D. M. & Rosen, M. R. Thrombin modulates phosphoinositide metabolism, cytosolic calcium, and impulse initiation in the heart. *Circ Res* **68**, 1216–1229 (1991).
57. Steinberg, S. F., Zhang, H., Pak, E., Pagnotta, G. & Boyden, P. A. Characteristics of the  $\beta$ -adrenergic receptor complex in the epicardial border zone of the 5-day infarcted canine heart. *Circulation* **91**, 2824–2833 (1995).
58. Steinberg, S. F., Robinson, R. B., Lieberman, H. B., Stern, D. M. & Rosen, M. R. Thrombin modulates phosphoinositide metabolism, cytosolic calcium, and impulse initiation in the heart. *Circ Res* **68**, 1216–1229 (1991).
59. Soto, D., De Arcangelis, V., Zhang, J. & Xiang, Y. Dynamic protein kinase A activities induced by  $\beta$ -adrenoceptors dictate signaling propagation for substrate phosphorylation and myocyte contraction. *Circ Res* **104**, 770–779 (2009).

## Acknowledgements

These studies were supported by NIH grants HL123061, HL127764 and HL112413.

## Author Contributions

M.P. and G.R.R. performed experiments; G.W. generated the anti- $\beta_1$ AR AABs; S.F.S. and Y.K.X. designed the experiments and interpreted the results. S.F.S. wrote the manuscript.

## Additional Information

**Supplementary information** accompanies this paper at doi:[10.1038/s41598-017-06607-z](https://doi.org/10.1038/s41598-017-06607-z)

**Competing Interests:** The authors declare that they have no competing interests.

**Publisher's note:** Springer Nature remains neutral with regard to jurisdictional claims in published maps and institutional affiliations.



**Open Access** This article is licensed under a Creative Commons Attribution 4.0 International License, which permits use, sharing, adaptation, distribution and reproduction in any medium or format, as long as you give appropriate credit to the original author(s) and the source, provide a link to the Creative Commons license, and indicate if changes were made. The images or other third party material in this article are included in the article's Creative Commons license, unless indicated otherwise in a credit line to the material. If material is not included in the article's Creative Commons license and your intended use is not permitted by statutory regulation or exceeds the permitted use, you will need to obtain permission directly from the copyright holder. To view a copy of this license, visit <http://creativecommons.org/licenses/by/4.0/>.

© The Author(s) 2017